Advances in Science and Technology Research Journal, 2025, 19(12), 361–369 https://doi.org/10.12913/22998624/210474 ISSN 2299-8624, License CC-BY 4.0

# Material inclusions and fiber orientation affect the aeroelastic stability of a composite wing

Balsam H. Abed¹, Khalid M. Sowoud¹, Emad Q. Hussein²

- <sup>1</sup> Aeronautical Technical Engineering Department, Al-Farahidi University, Baghdad 10011, Iraq
- <sup>2</sup> Petroleum Engineering Department, University of Kerbala, Karbala 56001, Iraq
- \* Corresponding author e-mail: khalid.sowoud@uoalfarahidi.edu.ig

#### **ABSTRACT**

This study investigates the effects of fiber orientation and inclusion materials (Al<sub>2</sub>O<sub>3</sub>), silica, and rubber) on the aeroelastic properties of a composite wing structure, including natural frequency, flutter speed, and damping ratio. A MATLAB-based model was created to analyze the dynamic responses, and the results were confirmed with ANSYS simulations. It was found that fiber orientation significantly influences structural dynamics, with zero fiber providing the highest natural frequency and flutter resistance; increasing the fiber angle reduces both. Adding Al<sub>2</sub>O<sub>3</sub> raised flutter speed by 10.8%, while rubber doubled the damping ratio compared to the pure composite at a 90° fiber orientation. Silica improved both damping and stiffness characteristics in a balanced way. These results are important for optimizing composite wing designs to improve aeroelastic performance across different flight conditions.

**Keywords:** composite material, material inclusions, sweep angle, taper ratio, flutter.

# INTRODUCTION

Composite materials have transformed aerospace structure design thanks to their high stiffnessto-weight ratios and design flexibility. However, the interaction of structural dynamics and aerodynamic forces, known as aeroelasticity, imposes significant design constraints such as flutter and divergence. Improving aeroelastic performance without increasing weight remains a major challenge [1]. Several studies looked into the aeroelastic behavior of composite wings, focusing on fiber orientation and geometric tailoring. The aeroelastic analysis of composite panels highlights their potential for passive flutter in flexible control [2]. The fundamentals of divergence and flutter for flexible airfoils were developed using panel methods. However, few studies have examined the use of additive materials such as rubber or ceramic particles in composite structures [3]. These questions have been widely used to forecast the effective material properties of composites containing inclusions. They investigated the effect of Nano-inclusion on

vibration properties but discovered no correlation with aeroelastic metrics [4, 5]. This study investigates how the inclusion of materials such as Al<sub>2</sub>O<sub>3</sub> (stiff ceramic), rubber (damping-enhancing elastomer), and silica (moderate filler) affects the effective stiffness and this study bridges the gap by explicitly modeling the effects of volume fraction-based inclusions on both dynamic and static aeroelastic instabilities in a composite wing. To evaluate the effect of different material inclusions and fiber orientations on the natural frequency, flutter speed, and damping behavior of composite panels, and to recommend the best configurations for improved aeroelastic performance.

Received: 2025.07.16

Accepted: 2025.10.01

Published: 2025.11.01

# **MATHEMATICAL MODEL**

A mathematical model and analysis of the vibration and flutter speed behavior of a composite wing panel with fiber orientation and material inclusions. The formulation analysis consists of [6, 7].

#### Effective elastic modulus with includes

To define a three-phase composite, we use the Voigt (rule of mixtures) approach. The longitudinal modulus  $E_1$  and effective density  $\rho$  are as follows:

$$E_1 = v_f E_f + v_m E_m + v_i E_i \tag{1}$$

$$\rho = v_f \rho_f + v_m \rho_m + v_i \rho_i \tag{2}$$

where:  $v_p$ ,  $v_m$ ,  $v_i$  – volume fraction of fiber, matrix and inclusion;  $E_p$ ,  $E_m$ ,  $E_i$  – elastic moduli of fiber, matrix and inclusion;  $p_p$ ,  $p_m$ ,  $p_i$  – densities of each phase.

The total stiffness matrices [A], [B], [D] [8]:

$$[A] = \sum_{k=1}^{N} Q_{ik}(z_k - z_{k-1})$$
 (3)

$$[B] = 1/2 \sum_{k=1}^{N} Q_{ik} (z_k^2 - z_{k-1}^2)$$
 (4)

$$[B] = 1/3 \sum_{k=1}^{N} Q_{ik} (z_k^3 - z_{k-1}^3)$$
 (5)

For a laminate with layers oriented at  $\theta_i$  calculate the transformed stiffness matrix for each ply.

$$\theta_i = T^{-1}|Q|T^{-T} \tag{6}$$

where: T – transformation matrix for rotation angle  $\theta_i$ , for a swept and tapered wing, using geometric transformations;

$$\bar{x} = x \cos(\Lambda) \tag{7}$$

$$y = y \left( \frac{1 - \lambda}{b} x + \lambda \right) \tag{8}$$

where:  $\Lambda$  – sweep angle;  $\lambda$  – taper ratio.

#### **Aerelastic flutter equations**

In matrix form, the generalized equations of motion can be expressed in three dimensions [9]:

$$\begin{bmatrix}
M_{h} & 0 & 0 \\
0 & M_{\theta} & 0 \\
0 & 0 & M_{\phi}
\end{bmatrix}
\begin{bmatrix}
\ddot{h} \\
\ddot{\theta} \\
\ddot{\theta}
\end{bmatrix} +
\begin{bmatrix}
C_{h} & 0 & 0 \\
0 & C_{\theta} & 0 \\
0 & 0 & C_{\phi}
\end{bmatrix}
\begin{bmatrix}
\dot{h} \\
\dot{\theta} \\
\dot{\phi}
\end{bmatrix} +$$

$$+
\begin{bmatrix}
K_{h} & 0 & 0 \\
0 & K_{\theta} & 0 \\
0 & 0 & K_{\phi}
\end{bmatrix}
\begin{bmatrix}
h \\
\theta \\
\phi
\end{bmatrix} =
\begin{bmatrix}
L \\
M \\
N
\end{bmatrix}$$
(9)

where:  $M_h$ ,  $M_{\theta}$ ,  $M_{\theta}$  are the mass moments for bending, torsion, and yaw, respectively,  $C_h$ ,  $C_{\theta}$ ,  $C_{\theta}$  are the damping coefficient,  $K_h$ ,  $K_{\theta}$ ,  $K_{\theta}$  are the stiffness coefficients for bending, torsion, and yaw modes are represented by [10], while L, M, and N denote the aerodynamic forces (lift, pitching moment, and yawing moment) acting on the wing.

# **Aerodynamic forces**

The aerodynamic forces acting on the wing depend on the angle of attack and the yaw angle. The lift and moment are influenced by these angles [11]:

$$L = \frac{1}{2}\rho V^2 SC_L(\alpha, \beta) \tag{10}$$

$$M = \frac{1}{2} \rho V^2 S \, c C_M(\alpha, \beta) \tag{11}$$

$$N = \frac{1}{2}\rho V^2 S \, cC_N(\alpha, \beta) \tag{12}$$

where:  $\rho$  represents the air density, V is the flight velocity, S is the wing area, and c is the mean aerodynamic chord. The coefficients  $C_L(\alpha, \beta)$ ,  $C_M(\alpha, \beta)$ , and  $C_N(\alpha, \beta)$  refer to the lift, pitch moment, and yaw moment, respectively. These coefficients are functions of the angle of attack  $(\alpha)$  and the yaw angle  $(\beta)$ .

### Coupled modes in flutter

Flutter is primarily caused by the interaction of bending and torsion modes. When damping becomes negative, this interaction generates dynamic instabilities, resulting in self-sustaining oscillations at the flutter point. The coupled equations that describe bending and torsion, taking into account aerodynamic forces, can be expressed as [12]:

$$M_h \ddot{h} + C_h \dot{h} + K_h h = L(\alpha, \beta) \tag{13}$$

$$M_{\theta}\ddot{\theta} + C_{\theta}\dot{\theta} + K_{\theta}\theta = M(\alpha, \beta) \tag{14}$$

The aerodynamic forces  $L(\alpha,\beta)$  and  $M(\alpha,\beta)$  depend on dynamic changes in  $\alpha$  and  $\beta$ , which vary based on the wing's motion. The flutter speed can be determined by solving the eigenvalue problem related to the equations of motion.

$$\det(\lambda^2 M + \lambda C + K) = 0 \tag{15}$$

where:  $\lambda$  represents the eigenvalues. The smallest value of  $\lambda$  determines the flutter speed, as the real part of the eigenvalue becomes negative, indicating instability.

## Case study

Determine the aeroelastic properties of a composite wing using MATLAB's best analytical predictions, which are then validated with an ANSYS simulation. The geometry and material properties of the wing study are presented in Table 1 [13–15].

#### **VALIDATION OF RESULT**

A thorough finite element analysis using AN-SYS was performed to validate the analytical predictions and investigate the composite wing panels' detailed dynamic behavior. The procedure was as follows: The wing panel geometry was modeled as a tapered, swept shell structure. Key dimensions such as span root and tip chord lengths, thickness, sweep angle, and aspect ratio were parametrically defined to match the study cases. Composite material properties were assigned based on orthotropic elasticity, and multiple material definitions were created to represent different inclusion configurations and fiber orientations. The model utilized Shell 181 elements, which are well-suited for composite layered structures. A mapped mesh was generated along the surface, with local mesh refinement near the root to capture high stress gradients. Mesh independence was verified by refining the model until the change in the first natural frequency was less than 2%. Cantilever boundary conditions were imposed, with the root edge of the wing fully fixed and the remaining edges free to simulate realistic

wing mounting. A block Lanczos eigenvalue extraction method was used to solve for natural frequencies, and the first five mode shapes were computed, with the first bending mode frequency recorded for comparison against the analytical results. Figure 1 shows the total deformation plot of the composite tapered wing panel's first bending mode shape at a natural frequency of 8.1 Hz, which was extracted from ANSYS modal analysis. The deformation pattern exhibits a typical first bending mode, with maximum displacement near the tip and minimal displacement at the root, consistent with cantilevered boundary conditions. The frequency obtained is consistent with the expected values for composite wing structures of comparable dimensions and stiffness properties. This visualization supplemented the numerical results by demonstrating that both material tailoring and geometric features are considered.

The wing panel has an aspect ratio of 6, and the fiber orientations range from 0° to 90°, as represented in Figure 2. The MATLAB model uses an analytical approach based on the Rayleigh-Ritz method, whereas ANSYS results are obtained through finite element model analysis. The results are plotted against fiber orientation, and as expected, both MATLAB and ANSYS results show a monotonic decrease in the first natural frequency as the fiber orientation angle increases. This behavior is explained by the gradual reduction in axial stiffness resulting from fiber misalignment in the principal load direction. At 0° orientation, the fibers are aligned with the loading axis, yielding a maximum natural frequency of approximately 8.1 Hz in ANSYS and 7.5 Hz in MATLAB. In contrast, at 90° degrees, the stiffness is reduced and the frequency falls to around 8.1 Hz in ANSYS and 2.0 Hz in MATLAB. The results show a high level of agreement between the two methods, with deviations of less than 7% over the entire orientation range. The greatest difference is observed at extreme fiber angles (0° and

Table 1. Shows the geometry and material properties of wing panels

Geometry and configuration	Material properties
Span length, L= 6 m	Elastic modulus, E <sub>1</sub> = 135 GPa
Root chord, C <sub>r</sub> = 1 m	Elastic modulus, E <sub>2</sub> = 10 GPa
Tip chord, C <sub>t</sub> = 0.6 m	Shear modulus, G <sub>12</sub> = 5 GPa
Sweep angle, $\Lambda$ = 0° to 45°	Poisson's ratio, v <sub>12</sub> = 0.3
Thickness, t = 0.057 m	Density,p = 1600 kg/m
Inclusion reinforcement 5% ${\sf Al_2O_3}$ , rubber and silica	

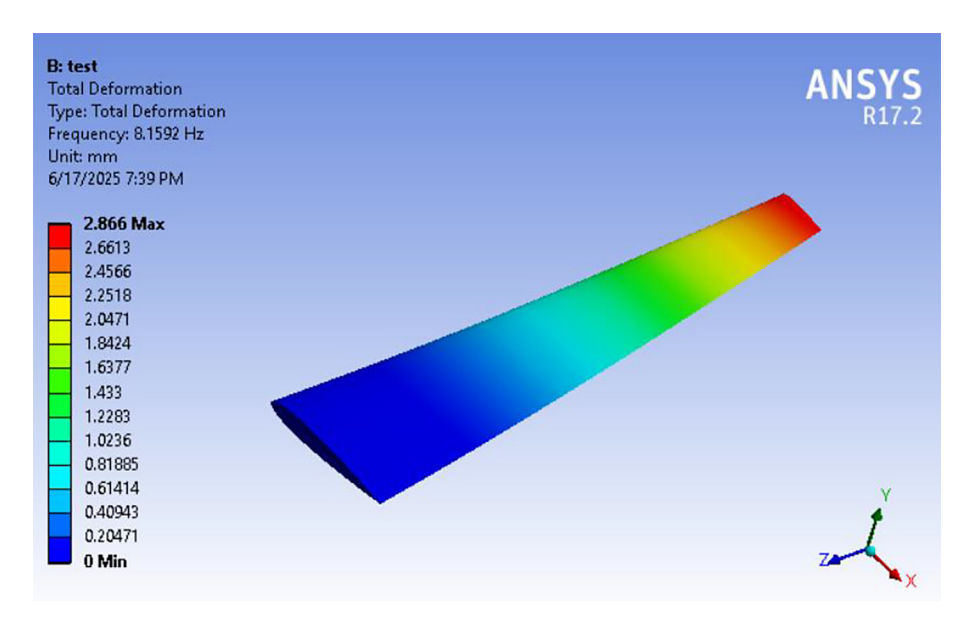


Figure 1. Counter for total deformation of the swept tapered wing

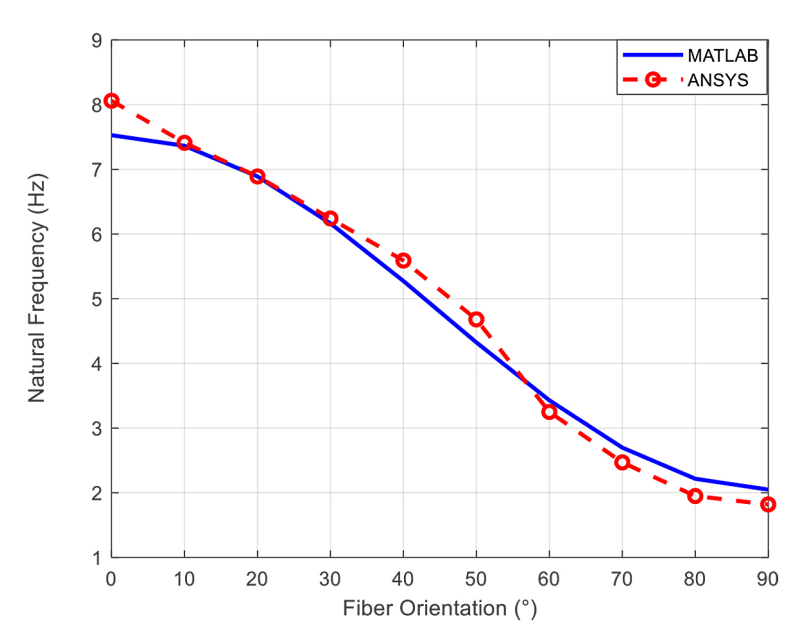


Figure 2. Natural frequency comparison MATLAB versus ANSYS

90°), which is most likely due to the analytical MATLAB model's simplified assumptions, such as uniform material distribution and ideal boundary conditions. Overall, the MATLAB model is useful for quick prediction and parametric studies, as well as getting accurate estimates of the first natural frequency for fiber orientation. The close match with ANSYS confirms the analytical approach, making it a valuable tool during the preliminary design phase.

Figure 3 compares the first five natural frequencies obtained from the MATLAB analytical model to those from ANSYS finite element

simulations. Each mode's frequencies are presented as bar charts. The figure clearly shows a strong correlation between all mode shapes. Notably, for the first mode, the frequencies are 7.5 Hz (MATLAB) versus 8.1 Hz (ANSYS), with minor differences that gradually increase for higher modes. However, these differences remain within a typical range of 2–5% variation, owing to the Rayleigh-Ritz method's simplified assumptions as opposed to detailed 3D finite element modeling. This strong agreement across multiple mode shapes validates the MATLAB approach's accuracy, demonstrating its suitability

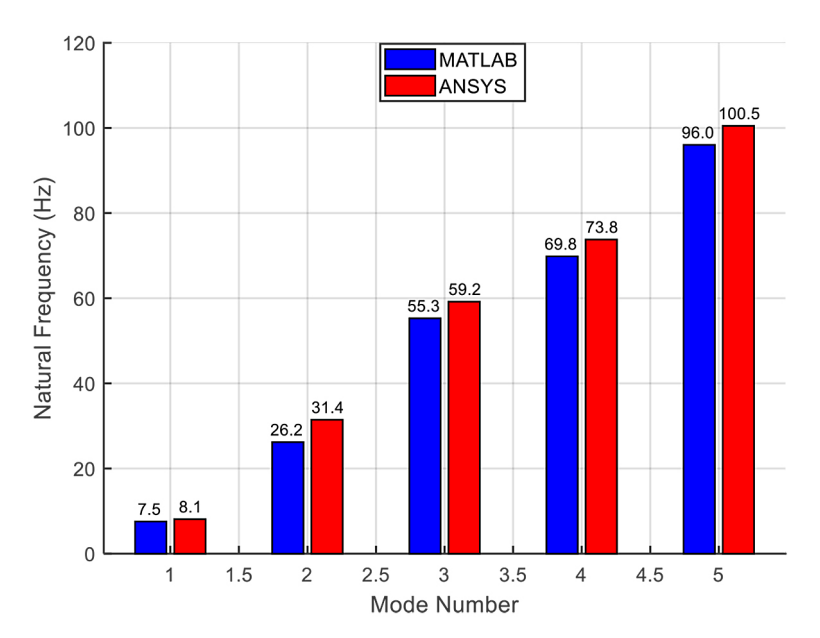


Figure 3. Bar chart for natural frequency in MATLAB versus ANSYS

for rapid parametric and optimization studies before engaging in computationally intensive finite element analyses.

#### **RESULT AND DISCUSSION**

This section presents a detailed investigation into the dynamic response of composite wing panels with varying fiber orientations and material inclusions. The study employs both an analytical approach implemented in MATLAB and finite element simulations carried out in ANSYS. It investigates how key parameters such as fiber angle, aspect ratio, taper ratio, sweep angle, and the inclusion of materials like Al<sub>2</sub>O<sub>3</sub>, rubber, and silica influence the composite structure's first natural frequency, flutter speed, and damping ratio. Figure 4 depicts how aspect ratio (AR = 4, 6, 8and 10) affects the first frequency of a composite wing panel as a function of fiber orientation angle  $(0 - 90^{\circ})$ . The results show a clear inverse relationship between fiber orientation angle and natural frequency across all aspect ratios. For each AR, the maximum frequency is observed at 0° fiber orientation (when the fibers align with the principal load direction), followed by a gradual decrease as the orientation approaches 90°, indicating a reduced contribution from the fibers in the bending direction. Lower aspect ratio wings (AR = 4) have significantly higher natural frequencies than higher aspect ratio wings (AR = 10), demonstrating the stiffening effect of shorter,

stubbier wings. For example, at 0° fiber orientation, AR = 4 generates a natural frequency greater than 10 Hz, whereas AR = 10 produces a frequency less than 1.5 Hz. This trend indicates that increasing the span relative to the chord leads to higher AR, greater structural flexibility, and thus lower vibrational stiffness. Furthermore, lower aspect ratios exhibit a faster rate of frequency decay with increasing fiber orientation. This implies that low AR structures are more prone to fiber misalignment, necessitating precise control over layup angles to maintain structural performance.

Figure 5 depicts the effect of taper ratio on the first natural frequency of a composite wing panel at various fiber orientation angles (0° to  $90^{\circ}$ ). The taper configurations were 0.4, 0.6, 0.8,and 1.0. The results clearly show that for all taper ratios, the natural frequency decreases with increasing fiber orientation angle, which corresponds to a decrease in longitudinal stiffness as fibers deviate from the primary load direction. Natural frequencies were highest in the most tapered configuration ( $\lambda = 0.4$ ), in which the wing narrows significantly near the tip. For example, at 0° fiber orientation, the natural frequency is approximately 2.17 Hz for the 0.4 taper case but decreases to around 1.5 Hz for the untapered  $(\lambda = 1)$  case. The increased frequency of more tapered wings can be attributed to a reduction in mass at the tip, which results in a stiffer dynamic response. Furthermore, as the taper ratio decreases, the natural frequency becomes more sensitive to fiber orientation. At 90° degrees

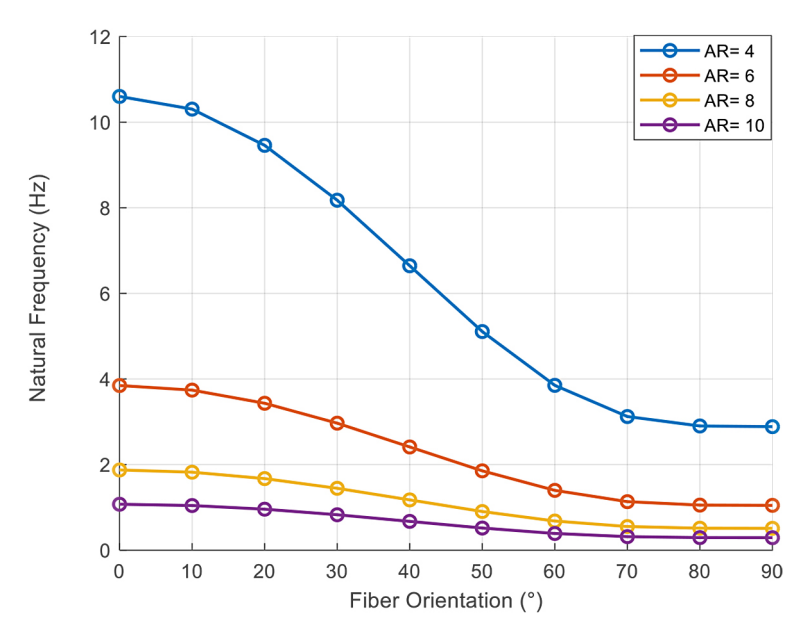


Figure 4. Effect of aspect ratio on natural frequency versus fiber orientation

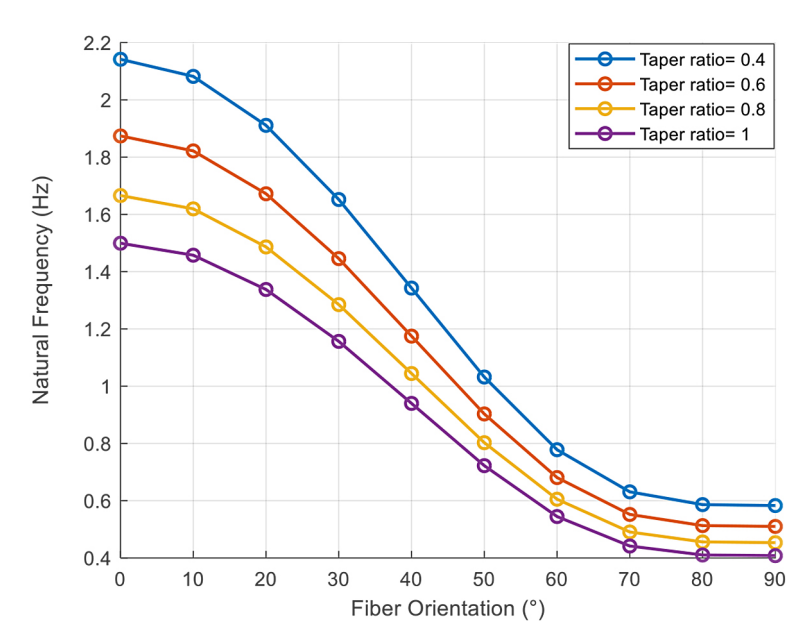


Figure 5. Effect of taper ratio on natural frequency versus fiber orientation

fiber orientation, the frequency variation among different tapers is narrower (ranging between 0.4 and 0.7 Hz), indicating that taper stiffening is more effective when fibers are aligned longitudinally. These findings indicate that incorporating taper into wing geometry can help increase natural frequency while potentially raising flutter margins. Designers should, however, carefully select taper ratios and fiber orientation to achieve the desired dynamic performance while maintaining aerolastic stability.

Figure 6 depicts the variation in the first natural frequency of a composite wing panel as

a function of fiber orientation angle at sweep angles of 0°, 15°, 30°, and 45°. In all cases, increasing the fiber orientation angle from 0° to 90° significantly reduces natural frequency. The most notable finding is a clear trend toward higher natural frequencies and wider sweep angles. At fiber orientation 0°, the natural frequency increases from about 2 Hz (no sweep) to around 4.8 Hz for a 45° sweep wing. This improvement is due to geometric stiffening caused by the swept plan form, which more evenly redistributes structural mass and stiffness in the chordwise and spanwise directions. Sweep has

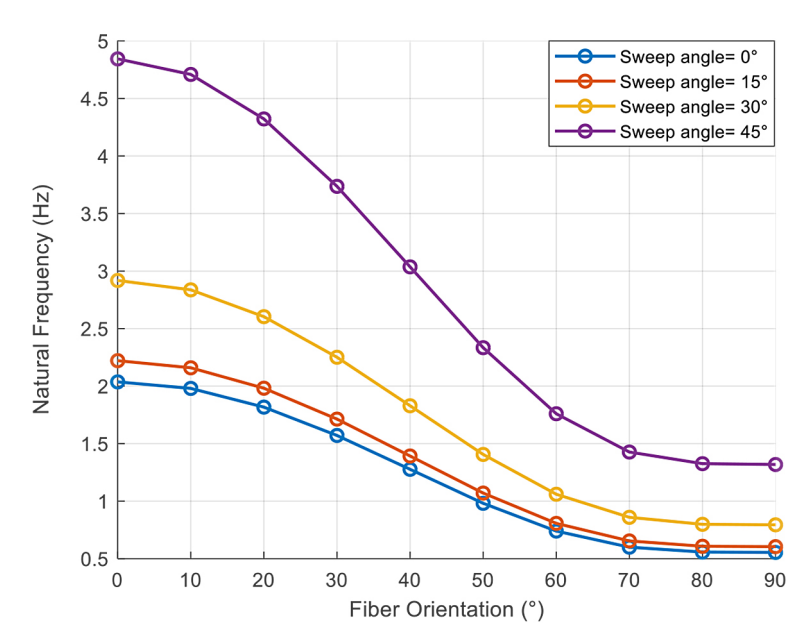


Figure 6. Effect of sweep angle on natural frequency versus fiber orientation

an especially strong effect at lower fiber angles. These findings indicate that sweep angle is an important design parameter not only for aerodynamics but also for structural dynamics, particularly in composite wings where fiber tailoring allows for finer tuning of vibrational properties.

Figure 7 depicts how flutter speed varies with fiber orientation angle for four configurations: pure composite and composites with  $Al_2O_3$ , rubber, and silica inclusions. The analysis reveals significant trends in aeroelastic stability across the entire fiber orientation range  $(0^{\circ}-90^{\circ})$ . Flutter speed decreases monotonically with increasing

fiber orientation across all material configurations. This is due to the gradual loss of axial and bending stiffness as fibers shift from longitudinal (0°) to transverse (90°) orientation, lowering the structural stiffness required to resist flutter. This configuration consistently has the highest flutter speed across all fiber angles, reaching up to 180 m/s at 0°. Al<sub>2</sub>O<sub>3</sub> increases stiffness due to its high elastic modulus, which improves aeroelastic performance. While using rubber, the lowest flutter speeds are observed here, starting at 110 m/s and decreasing significantly with increased orientation. This is because rubber has high damping but

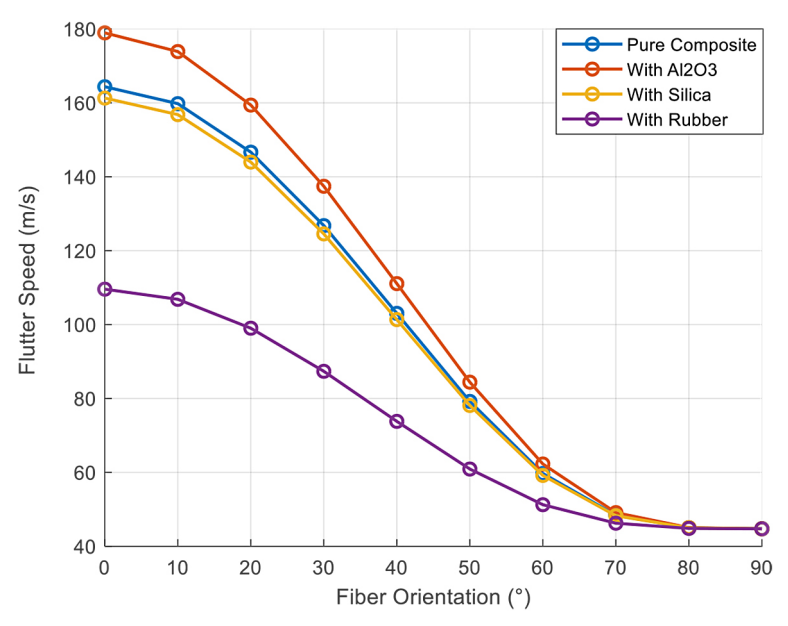


Figure 7. Flutter speed versus fiber orientation for various composite materials

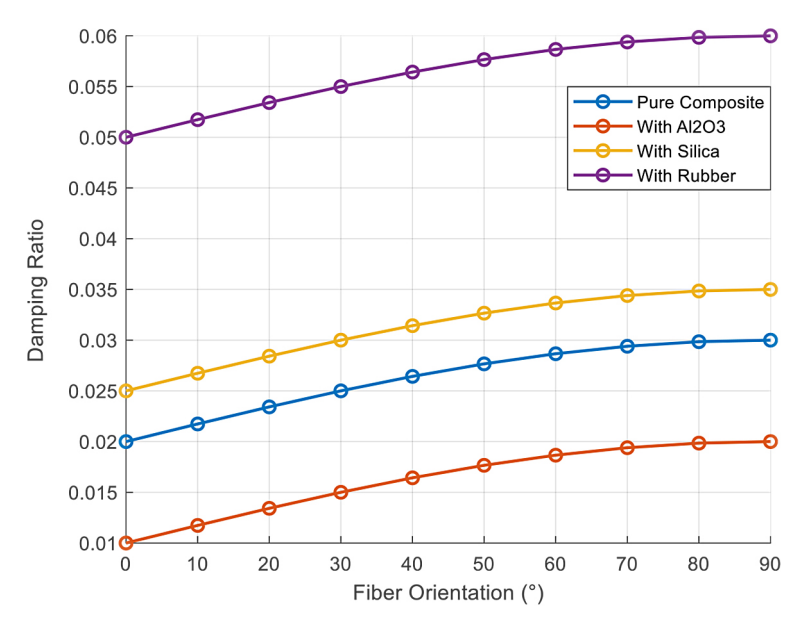


Figure 8. Damping ratio versus fiber orientation for various composite materials

low stiffness, which reduces structural rigidity and lowers the flutter threshold. The addition of stiff particles Al<sub>2</sub>O<sub>3</sub> significantly improves flutter resistance, especially at lower fiber angles.

Figure 8 illustrates the correlation between fiber orientation angles and estimated damping ratio for different composite material configurations, such as pure composites, composites with Al<sub>2</sub>O<sub>2</sub>, rubber, and silica inclusions. The damping ratio is a critical parameter that influences vibration attenuation and flutter margin in aeroelastic structures. The damping ratio for all material types gradually rises from 0° to 90° degrees of fiber orientation. This trend can be explained by the matrix's increased contribution in the transverse direction as fibers move away from the load-bearing axis, which enhances viscoelastic effects and energy dissipation. Rubber improves damping the most, but it may decrease flutter resistance. Al<sub>2</sub>O<sub>3</sub> is ideal for high stiffness and natural frequency, but has limited damping capability. This study demonstrates that fiber orientation and inclusion type have a significant impact on the damping properties of composite structures.

## **CONCLUSIONS**

This work investigated how fiber orientation and additive inclusions affect the aeroelastic response of composite wings. The MATLAB and ANSYS simulations yield several significant conclusions.

- Stiff inclusions (Al<sub>2</sub>O<sub>3</sub>) increase flutter speed and natural frequencies, making them ideal for high-speed, aeroelastic-sensitive applications.
- Rubber inclusions significantly improve damping for vibration suppression while decreasing critical speeds.
- Silica strikes a balance between stiffness and damping, providing moderate performance in both.

Furthermore, the interaction of fiber orientation and inclusion type can be used to design structural dynamics. To delay the onset of flutter, the best configurations strike a balance between stiffness, weight, and damping. As a result, the composite configuration can be customized to meet specific aeroelastic performance goals based on flight regime and structural constraints.

## **REFERENCES**

- Gennaretti, M., Morino, L. Fundamentals of Aeroelasticity. Springer. 2022. https://doi.org/10.1007/978-3-030-99973-5
- Hao, X., Tang, L., Meng, G. Aeroelastic analysis and flutter control of wings and panels: A review. Structural Control and Health Monitoring, 2016; 23(3): 409–435. https://doi.org/10.1002/stc.1780
- 3. Rajesh, S., et al. Dynamic characteristics of nano-SiC/epoxy composite plate: Experimental and numerical investigation. Polymer Testing, 2021; 101: 107295. https://doi.org/10.1016/j.polymertesting.2021.107295

- Suresh, S., Balaji, R., Anbazhagan, A. Effects of nanoinclusions on vibration characteristics of hybrid composites. materials today: Proceedings, 2020; 33: 2215
   2220. https://doi.org/10.1016/j.matpr.2020.05.251
- Ghiasi, H., Fayazbakhsh, K., Pasini, D., Lessard, L. Optimal design of composite panels under flutter and buckling constraints using lamination parameters. Composite Structures, 2017; 168: 28–36. https://doi.org/10.1016/j.compstruct.2017.02.045
- Fan, Z., et al. Vibration characteristics of variable stiffness composite wings. Composite Structures, 2022; 280: 114881. https://doi.org/10.1016/j. compstruct.2021.114881
- Zhang, D., Chen, D., Zhang, Y. Aeroelastic analysis of variable stiffness composite wings using nonlinear aerodynamic theory. Aerospace Science and Technology, 2020; 106: 106207. https://doi.org/10.1016/j.ast.2020.106207
- Kwon, H., Sankar, B. V. Flutter analysis of functionally graded composite wings. Mechanics of Advanced Materials and Structures, 2021; 28(4): 371–385. https:// doi.org/10.1080/15376494.2019.1611627
- Ullah, H., et al. Enhanced damping of composite structures using nano-rubber toughened epoxy matrices. Composite Part B: Engineering, 2021; 213: 108752. https://doi.org/10.1016/j.compositesb.2021.108752

- Song, Y., Kim, M. Multi-objective optimization of fiber orientation and material distribution in composite wings. Aerospace, 2023; 10(1): 35. https:// doi.org/10.3390/aerospace10010035
- 11. Wang, J., et al. Experimental flutter testing of composite panels with embedded damping layers. Journal of Sound and Vibration, 2022; 529: 116899. https://doi.org/10.1016/j.jsv.2022.116899
- Lee, D., Lee, I. Aeroelastic tailoring of composite wings for flutter suppression using layup optimization. Composite Structures, 2021; 256: 113107, https://doi.org/10.1016/j.compstruct.2020.113107
- 13. Mei, C., Dowell, E. H. Nonlinear aeroelastic analysis of composite wings using structural coupling and aerodynamic loads. Journal of Fluids and Structures, 2019; 89: 116–131. https://doi.org/10.1016/j.jfluidstructs.2019.05.006
- 14. Chen, H., Zhao, Y., Zhou, W. Design optimization of composite wing panels with damping enhancement using hybrid inclusions. Composite Part B: Engineering, 2022; 240: 109981. https://doi. org/10.1016/j.compositesb.2022.109981
- 15. Turkmen, M., Soykasap, O. Flutter suppression of advanced composite wings using variable fiber orientation and patch-wise reinforcement. Aerospace Science and Technology, 2023; 141: 108037. https:// doi.org/10.1016/j.ast.2023.108037